

## Contents

|  |    |
|--|----|
| Experimental details .....   | 1  |
| Material Synthesis.....  | 1  |
| Material characterization.....                                       | 2  |
| Catalytic experiments .....  | 3  |
| Results.....   | 5  |
| Characterization of new mixed metal Ce <sub>x</sub> /Zr-CAU-24 ..... | 5  |
| Catalysis .....  | 17 |

## Experimental details

### Material Synthesis

**Ce-UiO-66** was synthesized according to literature.<sup>1</sup> First, 177 mg (1.065 mmol) terephthalic acid was transferred to an 11 ml borosilicate glass reactor with magnetic stirring bar and dissolved in 6 ml DMF. To this, 2 ml of a 0.533 M aqueous cerium ammonium nitrate (CAN) solution was added. After closing, the reactor was immediately placed in a preheated heating block at 100°C for 15 minutes while being stirred at 500 rpm. The obtained precipitate was centrifuged and subsequently washed twice with 10 ml DMF and four times with 10 ml acetone.

**Zr-UiO-66** was synthesized by adapting a literature procedure.<sup>2</sup> First, 2.86 g (17.2 mmol) terephthalic acid and 2.00 g (8.6 mmol) zirconium tetrachloride were transferred to a 1 l glass Schott-bottle and dissolved in 150 ml DMF. To this, 1.5 ml of a 37 wt% HCl solution was added. After closing, the bottle was placed in a preheated synthesis oven at 120°C for 24 hours. The obtained precipitate was centrifuged and subsequently washed three times with 200 ml DMF and three times with 200 ml methanol.

**Ce-CAU-24** was synthesized according to literature.<sup>3</sup> First, 29.8 mg (53.3 μmol) 1,2,4,5-tetrakis(4-carboxyphenyl)benzene was introduced in an 8 ml Pyrex glass reaction tube with magnetic stirring bar and dissolved in 1.5 ml DMF. To this, 1.03 ml formic acid and 400 μl of a 1.066 M aqueous CAN solution was added. After closing, the reactor was immediately placed in a preheated heating block at 100°C for 15 minutes. The obtained precipitate was centrifuged and subsequently washed twice with 2 ml DMF and four times with 2 ml acetone.

**Zr-CAU-24** was synthesized according to literature.<sup>3</sup> First, 29.8 mg (53.3 μmol) 1,2,4,5-tetrakis(4-carboxyphenyl)benzene was introduced in an 8 ml Pyrex glass reaction tube with magnetic stirring bar and dissolved in 1.5 ml DMF. To this, 1.03 ml formic acid and 500 μl of a 0.533 M aqueous zirconyl nitrate hydrate solution was added. After closing, the reactor was immediately placed in a preheated heating block at 100°C for 15 minutes. The obtained precipitate was centrifuged and subsequently washed twice with 2 ml DMF and four times with 2 ml acetone.

**Ce<sub>10</sub>/Zr-UiO-66** was synthesized according to literature.<sup>4</sup> First, 127.6 mg (765 μmol) terephthalic acid was transferred to an 11 ml borosilicate glass reactor with magnetic stirring bar and dissolved in 3.6 ml DMF.

To this, 100  $\mu$ l of a 0.533 M aqueous CAN solution, 1100  $\mu$ l of a 0.533 M aqueous zirconyl nitrate oxyhydrate solution and 1.03 ml formic acid was added. After closing, the reactor was immediately placed in a preheated heating block at 100°C for 15 minutes while being stirred at 500 rpm. The obtained precipitate was centrifuged and subsequently washed twice with 10 ml DMF and four times with 10 ml acetone.

**Ce<sub>10</sub>/Zr-CAU-24** was synthesized by transferring 29.8 mg (53.3  $\mu$ mol) 1,2,4,5-tetrakis(4-carboxyphenyl)benzene to an 8 ml Pyrex glass reaction tube with magnetic stirring bar and dissolving it in 800  $\mu$ l DMF. To this, 40  $\mu$ l of a 0.533 M aqueous CAN solution, 360  $\mu$ l of a 0.533 M aqueous zirconyl nitrate oxyhydrate solution and 953  $\mu$ l formic acid was added. After closing, the reactor was immediately placed in a preheated heating block at 100°C for 15 minutes while being stirred at 500 rpm. The obtained precipitate was centrifuged and subsequently washed twice with 2 ml DMF and twice with 2 ml acetone.

**Ce<sub>16</sub>/Zr-CAU-24** (16 refers to the Ce:Zr ratio of 16:84) was synthesized by transferring 29.8 mg (53.3  $\mu$ mol) 1,2,4,5-tetrakis(4-carboxyphenyl)benzene to an 8 ml Pyrex glass reaction tube with magnetic stirring bar and dissolving it in 800  $\mu$ l DMF. To this, 80  $\mu$ l of a 0.533 M aqueous CAN solution, 320  $\mu$ l of a 0.533 M aqueous zirconyl nitrate oxyhydrate solution and 8763  $\mu$ l formic acid was added. After closing, the reactor was immediately placed in a preheated heating block at 100°C for 15 minutes while being stirred at 500 rpm. The obtained precipitate was centrifuged and subsequently washed twice with 2 ml DMF and twice with 2 ml acetone.

**Ce<sub>29</sub>/Zr-CAU-24** (29 refers to the Ce:Zr ratio of 29:71) was synthesized by transferring 29.8 mg (53.3  $\mu$ mol) 1,2,4,5-tetrakis(4-carboxyphenyl)benzene to an 8 ml Pyrex glass reaction tube with magnetic stirring bar and dissolving it in 800  $\mu$ l DMF. To this, 200  $\mu$ l of a 0.533 M aqueous CAN solution, 200  $\mu$ l of a 0.533 M aqueous zirconyl nitrate oxyhydrate solution and 644  $\mu$ l formic acid was added. After closing, the reactor was immediately placed in a preheated heating block at 100°C for 15 minutes while being stirred at 500 rpm. The obtained precipitate was centrifuged and subsequently washed twice with 2 ml DMF and twice with 2 ml acetone.

**Ce<sub>53</sub>/Zr-CAU-24** (53 refers to the Ce:Zr ratio of 53:47) was synthesized by transferring 29.8 mg (53.3  $\mu$ mol) 1,2,4,5-tetrakis(4-carboxyphenyl)benzene to an 8 ml Pyrex glass reaction tube with magnetic stirring bar and dissolving it in 800  $\mu$ l DMF. To this, 320  $\mu$ l of a 0.533 M aqueous CAN solution, 80  $\mu$ l of a 0.533 M aqueous zirconyl nitrate oxyhydrate solution and 412  $\mu$ l formic acid was added. After closing, the reactor was immediately placed in a preheated heating block at 100°C for 15 minutes while being stirred at 500 rpm. The obtained precipitate was centrifuged and subsequently washed twice with 2 ml DMF and twice with 2 ml acetone.

### Material characterization

Powder X-ray diffraction (PXRD) patterns were recorded on a Malvern PANalytical Empyrean diffractometer in transmission mode over a 1.3–45° 2 $\theta$  range, using a PIXcel3D solid state detector and Cu anode (Cu K $\alpha$ 1: 1.5406 Å; Cu K $\alpha$ 2: 1.5444 Å) or on a STOE Stadi MP diffractometer with a MYTHEN detector and monochromated CuK $\alpha$ 1 ( $\lambda$  = 1.5401 Å) radiation in transmission.

The cerium to zirconium ratio of the samples was determined by energy-dispersive X-ray (EDX) spectroscopy. The data were recorded on a Philips XL30 FEG microscope. Therefore the powder were prepared on a carbon foil and measured on three different spots to confirm the sample homogeneity.

Sorption experiments were performed using a BEL Japan Inc. Belsorpmax apparatus. Before the sorption experiments all compounds were heated at 160 °C under reduced pressure ( $10^{-2}$  kPa). The specific surface areas were determined using the Rouquerol method.<sup>5</sup>

Thermogravimetric measurements were carried out using Netzsch, STA-409CD under air flow (75 mL/min) with a heating rate of 4 K/min between 20 and 800 °C.

<sup>1</sup>H-NMR spectra were measured on a Bruker DRX 500 spectrometer. Before the <sup>1</sup>H-NMR measurements, the compounds were dissolved in a mixture of deuterated dimethyl sulfoxide (d<sub>6</sub>-DMSO) and 10 % deuteriochloric acid (DCI) in D<sub>2</sub>O (molar ratio 7:1).

The IR spectra were recorded on a Bruker ALPHA-FT-IR A220/D-01 spectrometer equipped with an ATR-unit.

### Catalytic experiments

To determine the SCR activity of Ce-UiO-66, a reaction was performed in a fixed-bed quartz reactor (internal diameter: 3 mm) loaded with 200 mg catalyst (mesh 35-60). Prior to reaction, the catalyst was pretreated at 180°C under a 30 ml/min N<sub>2</sub> flow for 8 hours (ramp: 5°C/min) and allowed to cool down to 100°C. The inlet concentration was accurately measured by bypassing the reactor for 2 hours. Afterwards, the reactor's temperature was stepwise increased with isothermal plateaus of 2 hours to guarantee steady-state conditions. The total flow over the reactor was 30 ml/min, corresponding to a gas hourly space velocity (GHSV) of approximately 9000 h<sup>-1</sup>. The typical reaction gas mixture contained 500 ppm NO, 500 ppm NH<sub>3</sub>, 10 % O<sub>2</sub> and balance N<sub>2</sub>. The reactor outlet was diluted with 120 ml/min N<sub>2</sub> to allow a fast response of the FTIR gas analyzer. All other catalysts were tested analogously by loading an equimolar metal amount.

The reaction orders were determined similarly: a fixed-bed quartz reactor (internal diameter: 3 mm) was loaded with 200 mg Ce-UiO-66, Ce<sub>10</sub>/Zr-CAU-24 or 1000 mg CeO<sub>2</sub> (mesh 35-60). Prior to reaction, the catalyst was pretreated at 180°C under a 30 ml/min N<sub>2</sub> flow for 8 hours (ramp: 5°C/min) and further heated to 210°C. The absolute conversion was accurately measured by bypassing the reactor for 2 hours and subsequently sending the gas mixture over the catalyst bed for 2 hours. Reaction in absence of one of the reagents was performed in the same series as the reaction order of these reagents. A total flow of 150 ml/min (Ce-UiO-66 and CeO<sub>2</sub>) or 50 ml/min (Ce<sub>10</sub>/Zr-CAU-24) was maintained and the standard inlet concentrations were 500 ppm NO, 500 ppm NH<sub>3</sub> and 10% O<sub>2</sub> in nitrogen.

The ammonia adsorption was quantified in the same setup: a fixed-bed quartz reactor (internal diameter: 3 mm) was loaded with 200 mg Ce-UiO-66 (or equimolar amount of other MOFs) or 1000 mg CeO<sub>2</sub> (mesh 35-60). Prior to adsorption, the materials were pretreated at 180°C under a 30 ml/min N<sub>2</sub> flow for 8 hours (ramp: 5°C/min) and allowed to cool down to 100°C. Then, the inlet NH<sub>3</sub> concentration was determined by bypassing the reactor for 2 hours. Afterwards, the gas stream was sent over the reactor and the reactor's temperature was stepwise increased with isothermal plateaus of 2 hours to guarantee steady-state conditions. The typical gas stream contained 500 ppm NH<sub>3</sub> and balance N<sub>2</sub>. The reactor outlet was diluted with 120 ml/min N<sub>2</sub> to allow a fast response of the FTIR gas analyzer. The ammonia adsorption was quantified by integrating the difference between inlet and outlet concentration over time (see figure S1).

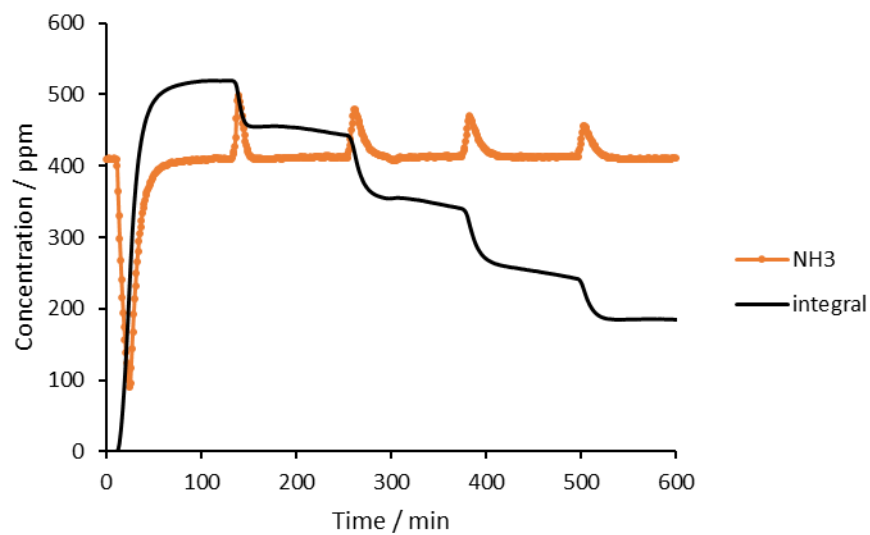


**Figure S1.** Example of ammonia adsorption experiment. The ammonia adsorption capacity is determined by integrating the difference between inlet concentration (here: 410 ppm) and outlet concentration. Initially, the reactor is bypassed and after 10 minutes, the gas stream is sent to the reactor. The temperature is stepwise increased every 120 minutes. Integral in arbitrary units.

## Results

### Characterization of new mixed metal Ce<sub>x</sub>/Zr-CAU-24

*Powder X-ray diffraction.*

The crystallographic data and phase purity of the different Ce<sub>x</sub>/Zr-CAU-24 materials were confirmed by the Le Bail method (Table S1. and Figure S2-5). Potassium chloride was used as internal standard.

**Table S1.** Overview of the crystallographic data of the mixed-metal compounds compared to the literature of Ce- and Zr-CAU-24.

| Compound                    | Space group | Lattice parameter / Å                                 | $r_{wp}$ / % | GoF  |
|-----------------------------|-------------|---|--------------|------|
| Zr-CAU-24 <sup>3</sup>      | <i>Cmmm</i> | $a = 20.141(2)$<br>$b = 34.89(1)$<br>$c = 11.1939(7)$ | 1.91         | 3.38 |
| Ce <sub>10</sub> /Zr-CAU-24 | <i>Cmmm</i> | $a = 19.947(3)$<br>$b = 34.958(5)$<br>$c = 11.851(1)$ | 3.38         | 2.12 |
| Ce <sub>16</sub> /Zr-CAU-24 | <i>Cmmm</i> | $a = 19.981(7)$<br>$b = 34.883(6)$<br>$c = 11.897(2)$ | 5.63         | 3.63 |
| Ce <sub>29</sub> /Zr-CAU-24 | <i>Cmmm</i> | $a = 20.057(4)$<br>$b = 35.113(5)$<br>$c = 12.053(2)$ | 4.99         | 3.00 |
| Ce <sub>53</sub> /Zr-CAU-24 | <i>Cmmm</i> | $a = 19.977(6)$<br>$b = 34.929(7)$<br>$c = 12.275(3)$ | 4.26         | 2.40 |
| Ce-CAU-24 <sup>3</sup>      | <i>Cmmm</i> | $a = 20.099(6)$<br>$b = 35.19(1)$<br>$c = 11.778(2)$  | 1.61         | 3.30 |

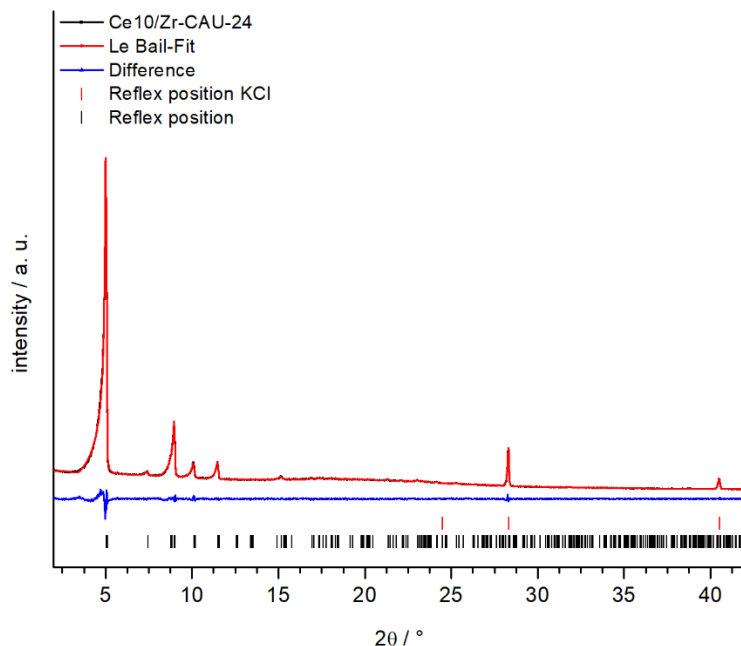


**Figure S2.** Le Bail plot of the mixed-metal compound Ce<sub>10</sub>/Zr-CAU-24. The observed PXRD pattern is shown in black, the calculated in red and the difference (observed - calculated) is given in blue. The allowed reflection positions are given as black and red (KCl) ticks.

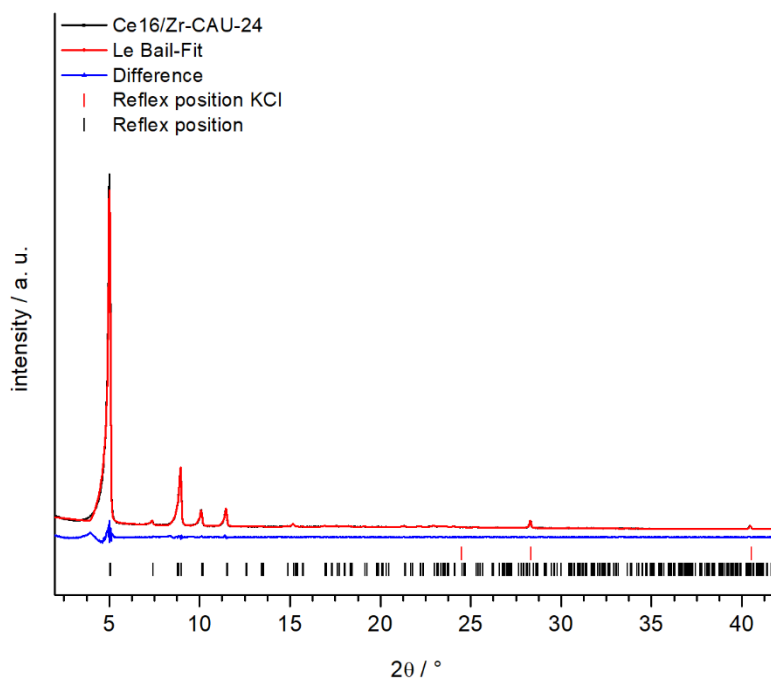


**Figure S3.** Le Bail plot of the mixed-metal compound Ce<sub>16</sub>/Zr-CAU-24. The observed PXRD pattern is shown in black, the calculated in red and the difference (observed - calculated) is given in blue. The allowed reflection positions are given as black and red (KCl) ticks.

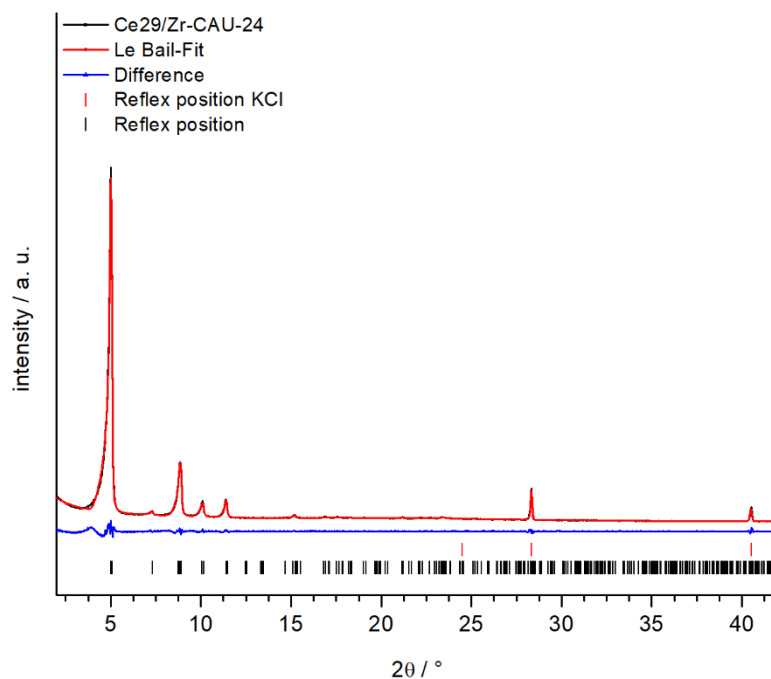


**Figure S4.** Le Bail plot of the mixed-metal compound Ce<sub>29</sub>/Zr-CAU-24. The observed PXRD pattern is shown in black, the calculated in red and the difference (observed - calculated) is given in blue. The allowed reflex positions of the peaks are given as black and red (KCl) tics.

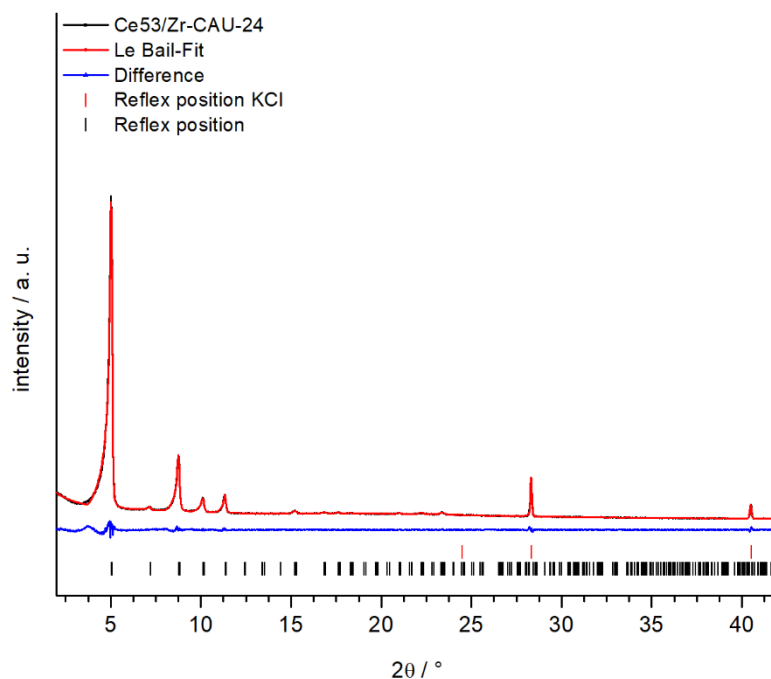


**Figure S5.** Le Bail plot of the mixed-metal compound Ce<sub>53</sub>/Zr-CAU-24. The observed PXRD pattern is shown in black, the calculated in red and the difference (observed - calculated) is given in blue. The allowed reflex positions of the peaks are given as black and red (KCl) tics.

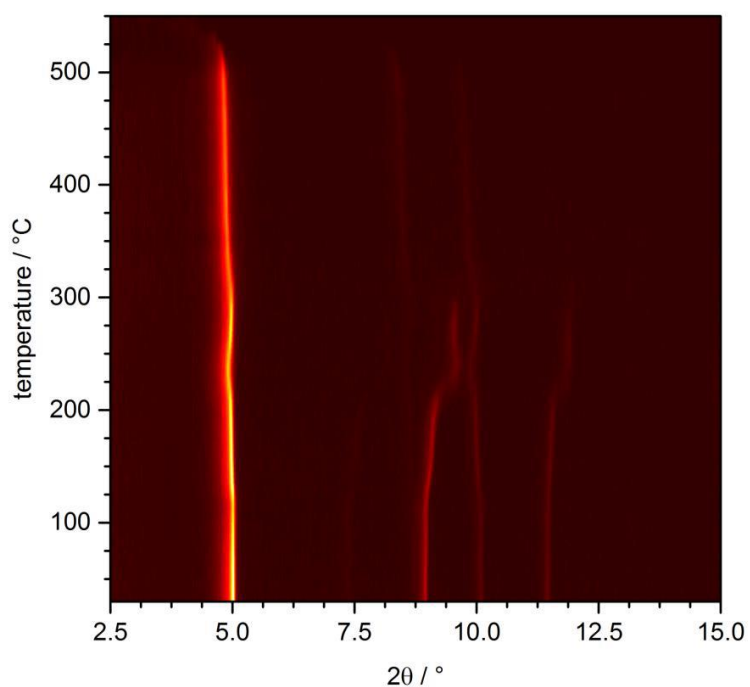


**Figure S6.** Variable temperature powder diffraction of Ce<sub>10</sub>/Zr-CAU-24 demonstrating that the material is stable up to approximately 300°C. The phase transformation at 220°C is attributed to the loss of solvent molecules, as has been described for Zr-CAU-24.<sup>3</sup>

### Elemental analysis

**Table S2.** The cerium to zirconium ratio in the Ce<sub>x</sub>/Zr-CAU-24 materials as determined by EDX.

| Sample                      | Ce content / at% |       |       | Mean         | Standard deviation / at% |
|-----------------------------|------------------|-------|-------|--------------|--------------------------|
|                             | (1)              | (2)   | (3)   |              |                          |
| Ce <sub>10</sub> /Zr-CAU-24 | 10.25            | 8.44  | 10.87 | <b>9.85</b>  | 1.03                     |
| Ce <sub>16</sub> /Zr-CAU-24 | 15.89            | 15.78 | 16.08 | <b>15.92</b> | 0.12                     |
| Ce <sub>29</sub> /Zr-CAU-24 | 28.97            | 28.66 | 29.91 | <b>29.18</b> | 0.53                     |
| Ce <sub>53</sub> /Zr-CAU-24 | 52.56            | 52.67 | 53.96 | <b>53.06</b> | 0.64                     |

### N<sub>2</sub> physisorption

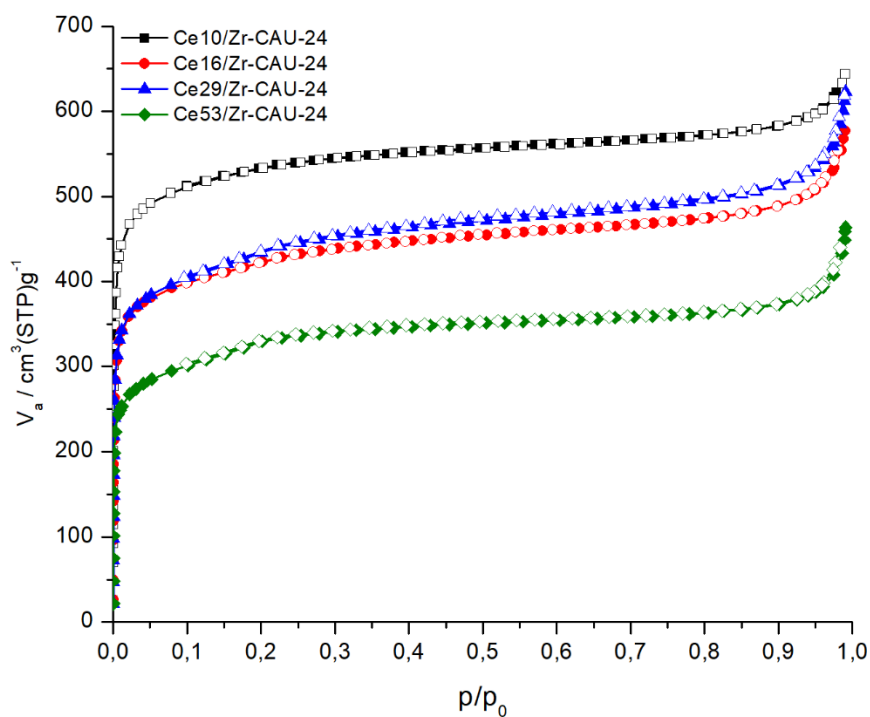


**Figure S7.** Results of N<sub>2</sub> sorption measurements of the Ce<sub>x</sub>/Zr-CAU-24 mixed-metal compounds. All compounds were activated at 160 °C under reduced pressure (10<sup>-2</sup> kPa). The filled symbols mark the adsorption isotherm, the empty symbols mark the desorption isotherm.

**Table S3.** Specific surface area and pore volume of the Ce<sub>x</sub>/Zr-CAU-24 materials.

| Compound                    | mass / g mol <sup>-1</sup> | S <sub>BET</sub> / m <sup>2</sup> g <sup>-1</sup> | S <sub>BET</sub> / m <sup>2</sup> μmol <sup>-1</sup> | Pore volume / cm <sup>3</sup> g <sup>-1</sup> |
|-----------------------------|----------------------------|---|--|---|
| Ce <sub>10</sub> /Zr-CAU-24 | 1407                       | 2056  | 2.89   | 0.861   |
| Ce <sub>16</sub> /Zr-CAU-24 | 1425                       | 1584  | 2.26   | 0.702   |
| Ce <sub>29</sub> /Zr-CAU-24 | 1463                       | 1613  | 2.36   | 0.723   |
| Ce <sub>53</sub> /Zr-CAU-24 | 1534                       | 1183  | 1.82   | 0.543   |

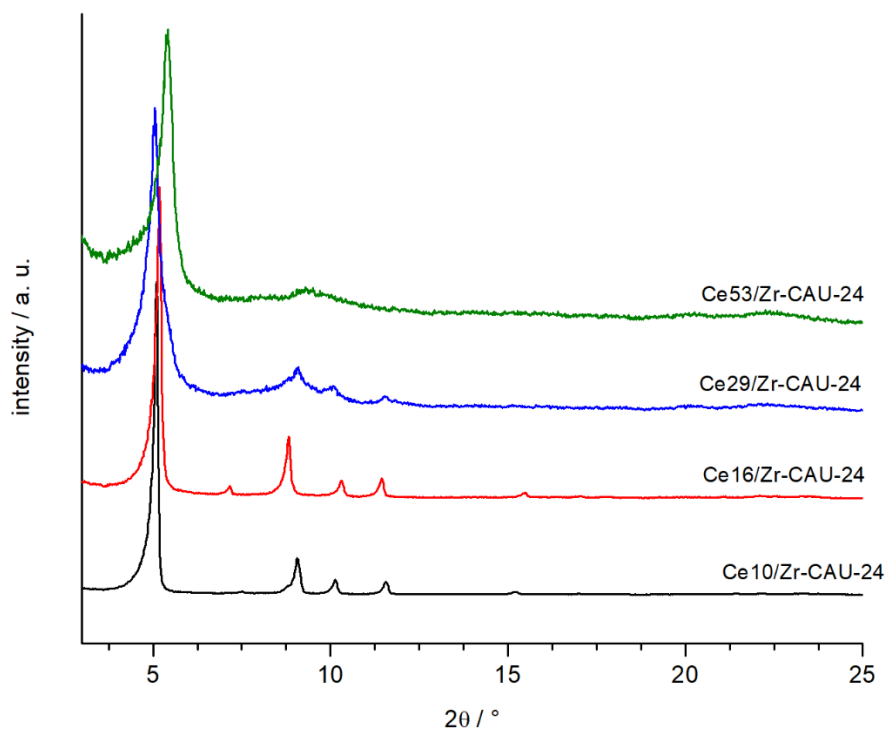


**Figure S8.** PXRD patterns of the  $\text{Ce}_x/\text{Zr-CAU-24}$  materials after  $\text{N}_2$  physisorption experiments.

*Thermogravimetric analysis*

**Table S4.** Overview of the TG analysis results. The temperature ranges of the individual decomposition steps and the corresponding mass losses are given. The agreement between the determined and ideal linker per cluster ratio are given.

| Compound                        | $\text{Ce}_{10}/\text{Zr-CAU-24}$ | $\text{Ce}_{16}/\text{Zr-CAU-24}$ | $\text{Ce}_{29}/\text{Zr-CAU-24}$ | $\text{Ce}_{53}/\text{Zr-CAU-24}$ |
|---------------------------------|-----------------------------------|-----------------------------------|-----------------------------------|-----------------------------------|
| Temperature / °C                | 25 - 335                          | 25 - 332                          | 25 - 301                          | 25 - 298                          |
| Mass loss / %                   | 15.04                             | 18.41                             | 19.88                             | 16.47                             |
| Temperature / °C                | 335 - 800                         | 332 - 800                         | 301 - 800                         | 298 - 800                         |
| Mass loss / %                   | 49.57                             | 48.85                             | 49.48                             | 48.27                             |
| Residual mass / %               | 33.26                             | 32.83                             | 30.94                             | 35.26                             |
| Determined Linker:cluster ratio | 2.0                               | 2.1                               | 2.2                               | 2.3                               |
| Ideal Linker:cluster ratio      | 2.0                               | 2.0                               | 2.0                               | 2.0                               |

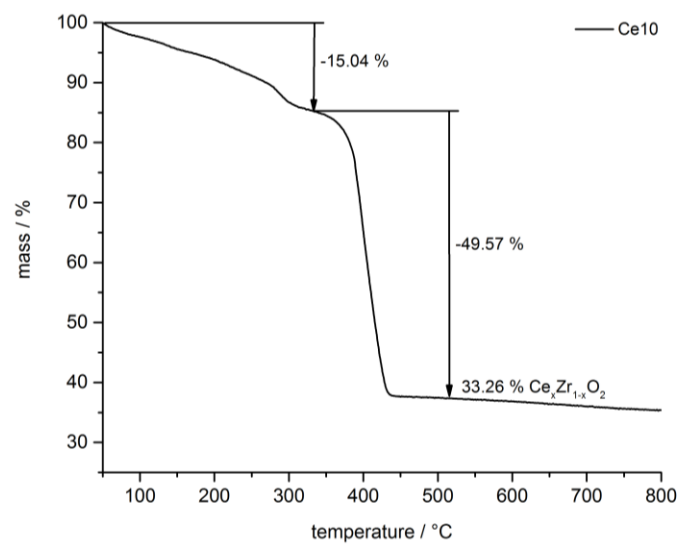


**Figure S9.** TGA of Ce<sub>10</sub>/Zr-CAU-24 under air.

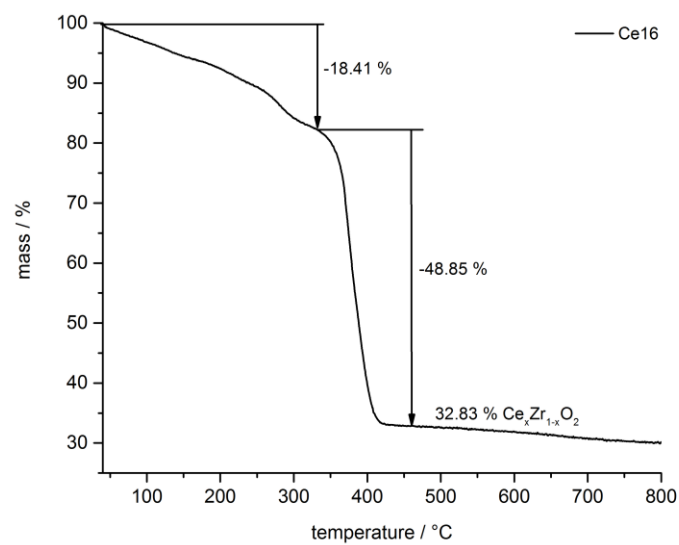


**Figure S10.** TGA of Ce<sub>16</sub>/Zr-CAU-24 under air.

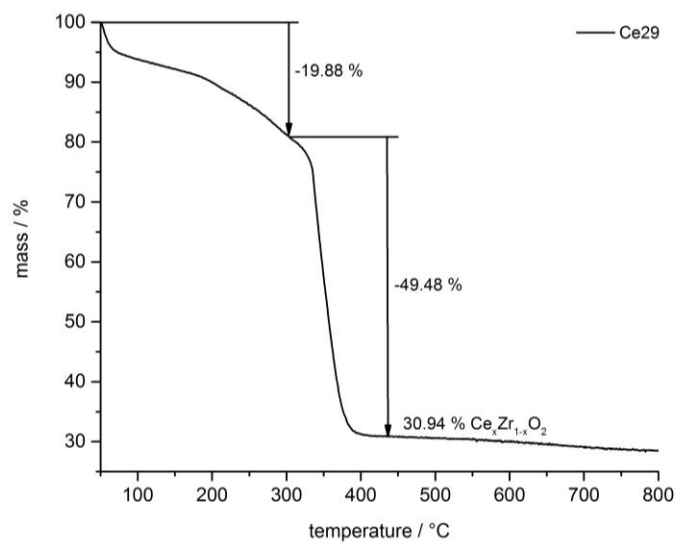


**Figure S11.** TGA of Ce<sub>29</sub>/Zr-CAU-24 under air.

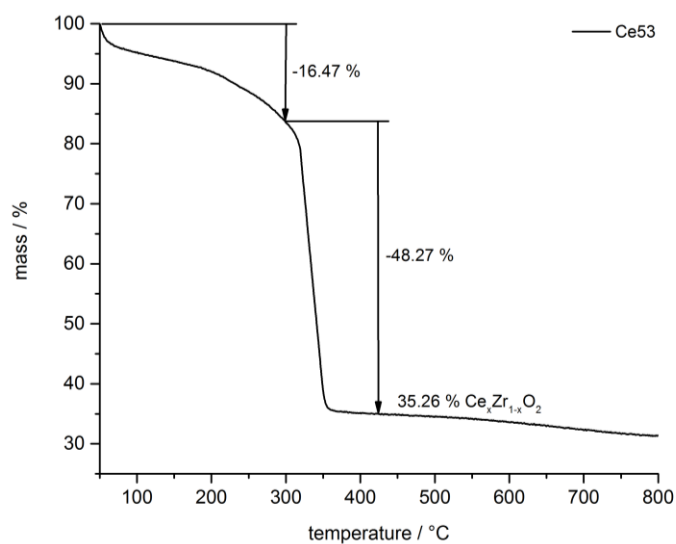


**Figure S12.** TGA of Ce<sub>53</sub>/Zr-CAU-24 under air.

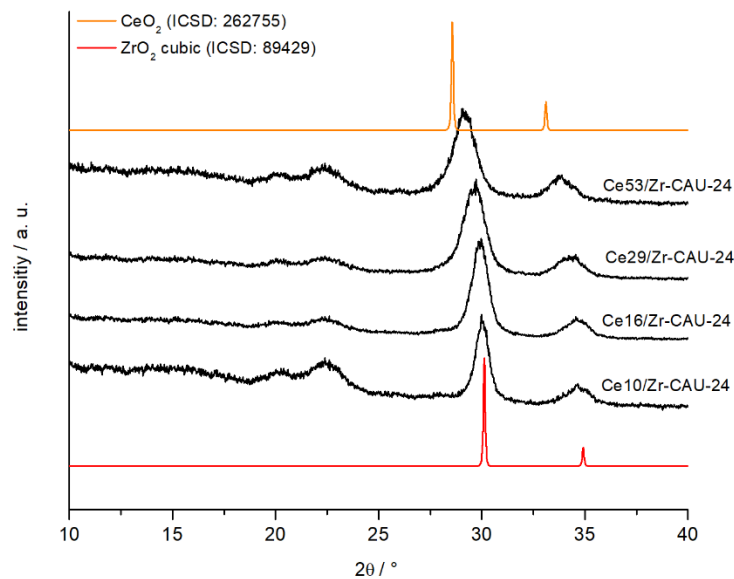


**Figure S13.** PXRD patterns of the  $\text{Ce}_x/\text{Zr-CAU-24}$  materials compared to  $\text{CeO}_2$  and  $\text{ZrO}_2$ , demonstrating that the mixed metal MOFs decompose to mixed metal oxides.

*NMR spectroscopy*

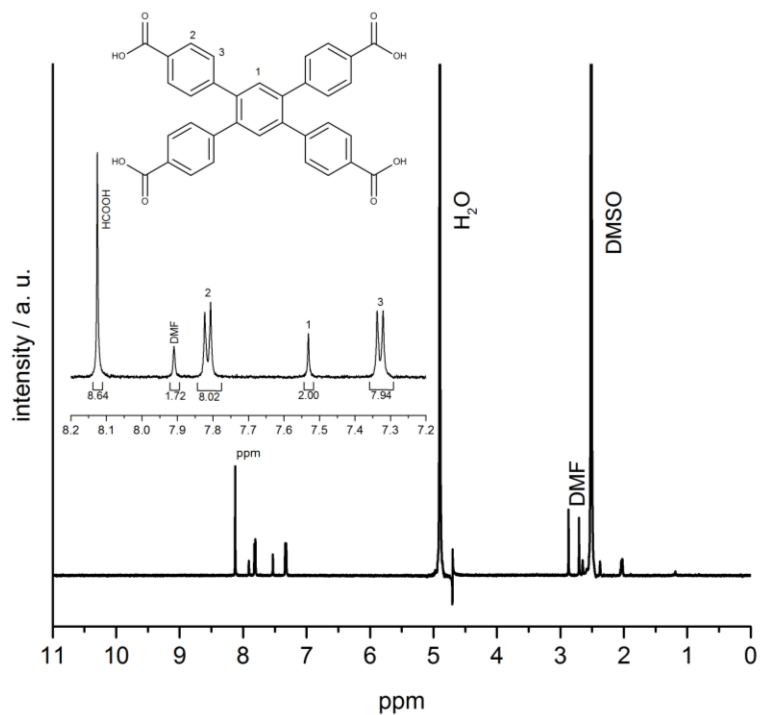


**Figure S14.**  $^1\text{H}$ -NMR of  $\text{Ce}_{10}/\text{Zr-CAU-24}$  dissolved in  $d_6$ -DMSO.

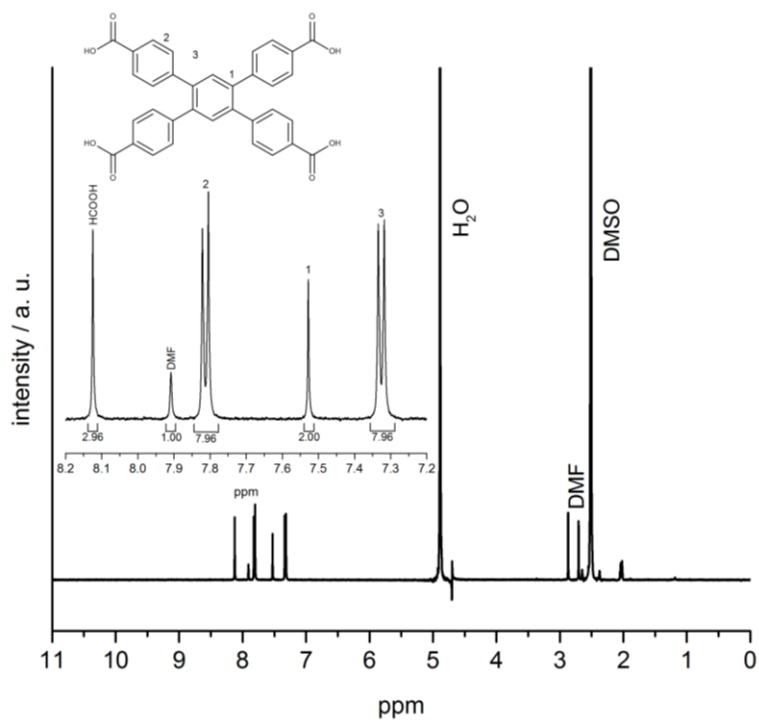


**Figure S15.**  $^1\text{H}$ -NMR of  $\text{Ce}_{16}/\text{Zr-CAU-24}$  dissolved in  $\text{d}_6$ -DMSO.

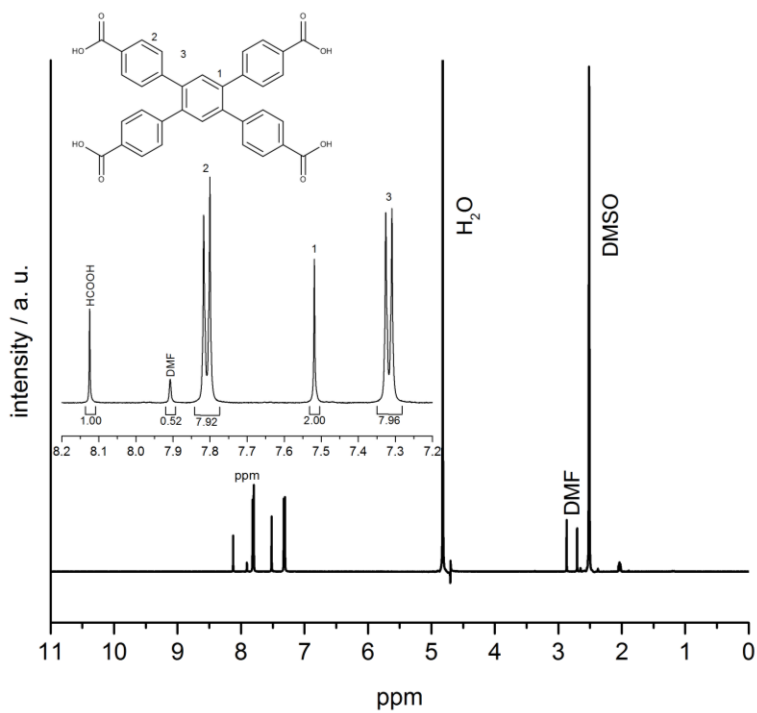


**Figure S16.**  $^1\text{H}$ -NMR of  $\text{Ce}_{29}/\text{Zr-CAU-24}$  dissolved in  $\text{d}_6$ -DMSO.

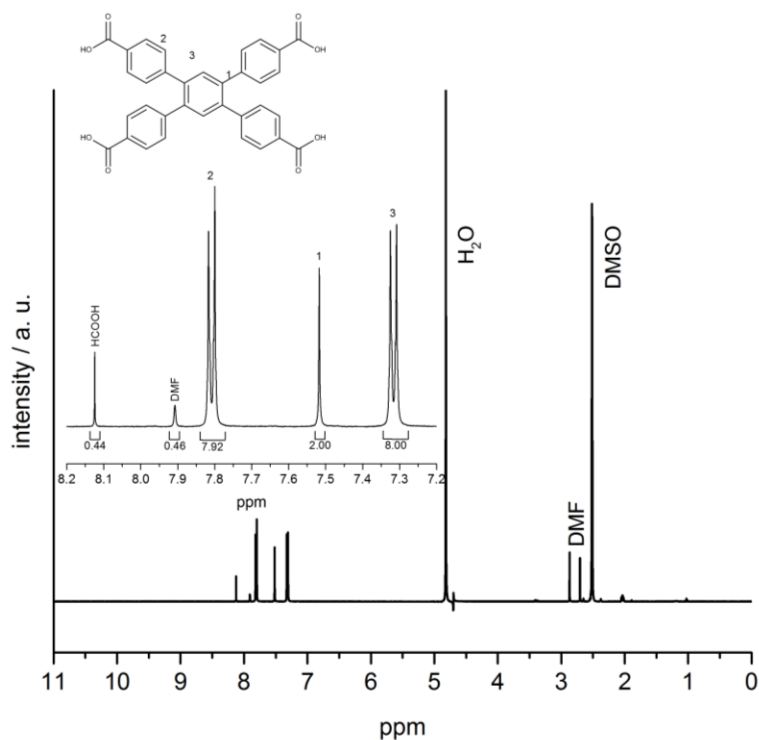


**Figure S17.**  $^1\text{H}$ -NMR of  $\text{Ce}_{53}/\text{Zr-CAU-24}$  dissolved in  $\text{d}_6$ -DMSO.

#### IR spectroscopy

By IR spectroscopy the remaining solvent and modulator molecules were detected and the known bands from the literature were confirmed.<sup>3</sup> The IR spectra are given in Figure S18 and the bands are summarized in Table S5. In the spectra only the expected bands of the linker and solvent molecules were detected. These results are in line with the results of the  $^1\text{H}$ -NMR spectra.

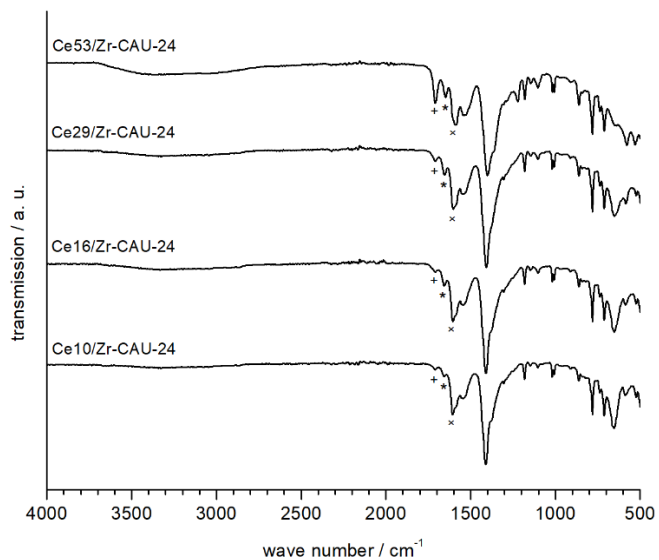


**Figure S18.** IR spectra of the  $\text{Ce}_x/\text{Zr-CAU-24}$  materials. The bands of the solvent molecules acetone (+), DMF (\*) and formic acid (x) are marked.

**Table S5.** Summary of the IR bands of the Ce<sub>x</sub>/Zr-CAU-24 materials based on literature.<sup>3</sup>

| IR-Band /cm <sup>-1</sup> | Kind of vibration                    |
|---------------------------|--------------------------------------|
| 1711                      | <i>ν</i> <sub>acetone</sub> (C=O)    |
| 1653                      | <i>ν</i> <sub>DMF</sub> (C=O)        |
| 1605                      | <i>ν</i> <sub>fomic acid</sub> (C=O) |
| 1587                      | <i>ν</i> <sub>as</sub> (COO-)        |
| 1543, 1526                | <i>ν</i> (C=C)                       |
| 1409                      | <i>ν</i> <sub>s</sub> (COO-)         |
| 860, 781                  | <i>ν</i> (C-H)                       |
| 654                       | <i>ν</i> (Zr-O)                      |
| 582                       | <i>ν</i> (Ce-O)                      |

## Catalysis

All MOF catalysts were tested up to their thermal stability limit. This was determined by measuring PXRD patterns after reaction, which demonstrated the decreased, but still present, crystallinity of the materials (Figure S19-22).

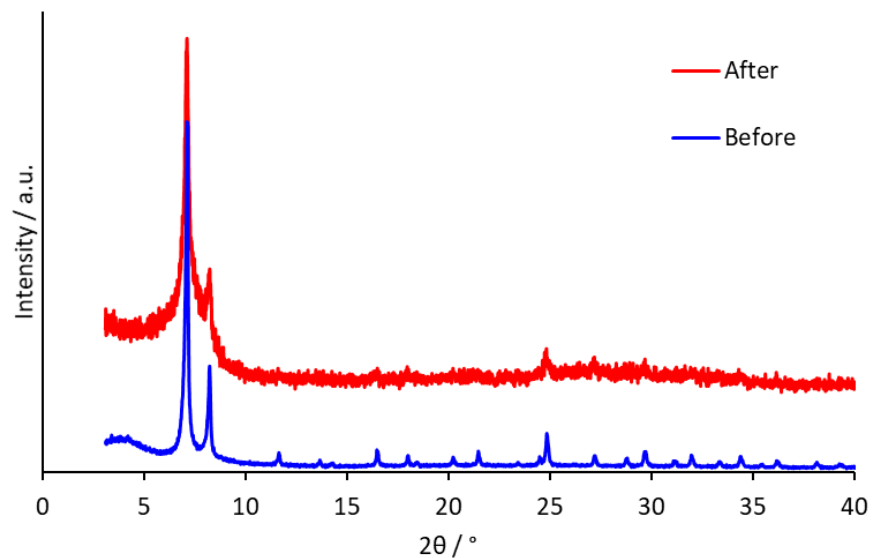


**Figure S19.** PXRD pattern of Ce-UiO-66 before (blue) and after (red) reaction.

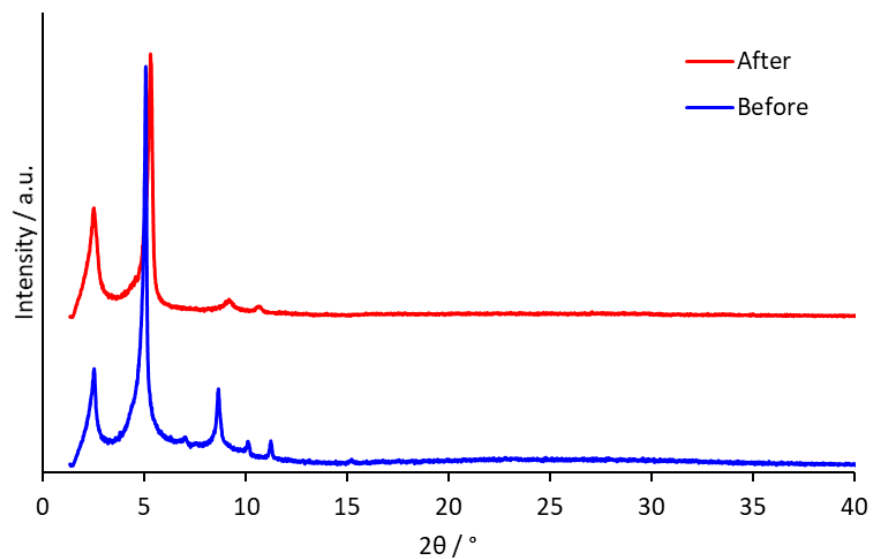


**Figure S20.** PXRD pattern of Ce-CAU-24 before (blue) and after (red) reaction.

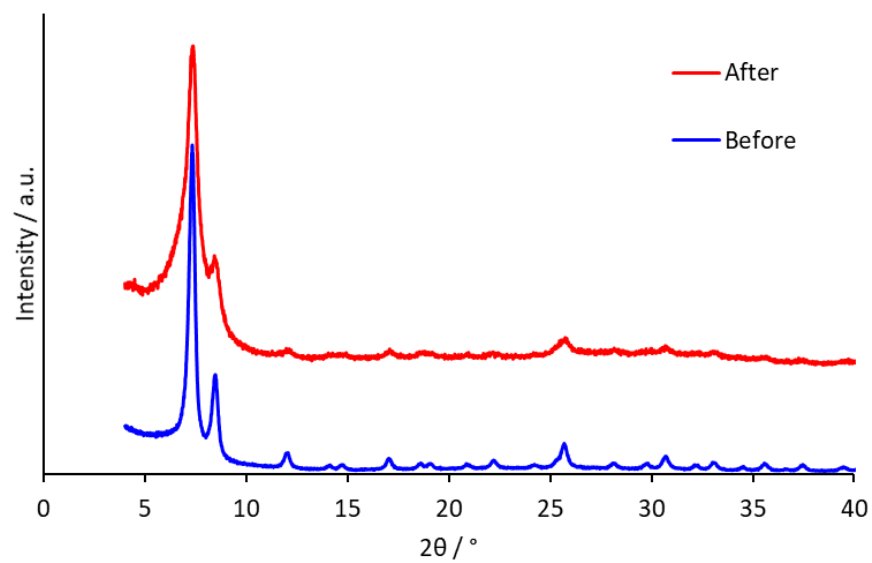


**Figure S21.** PXRD pattern of Ce<sub>10</sub>/Zr-UiO-66 before (blue) and after (red) reaction.

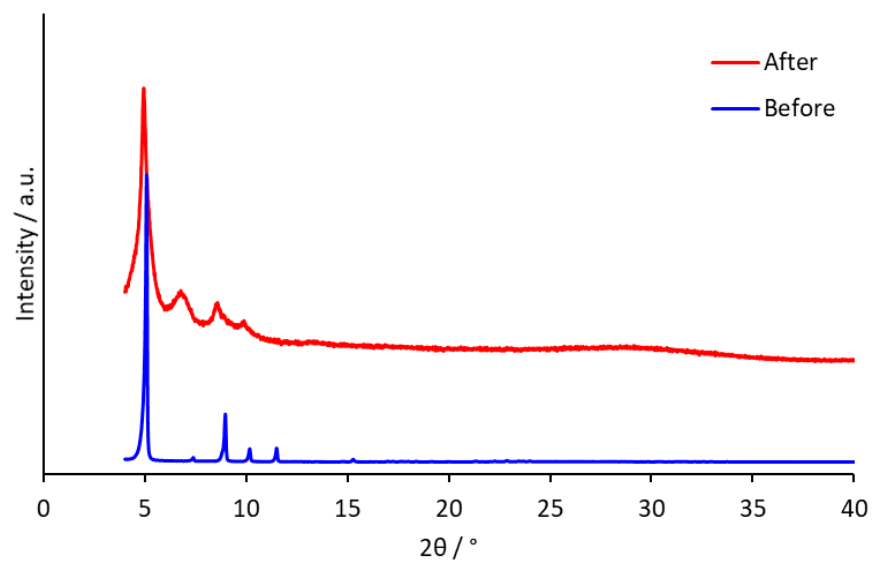


**Figure S22.** PXRD pattern of Ce<sub>10</sub>/Zr-CAU-24 before (blue) and after (red) reaction.

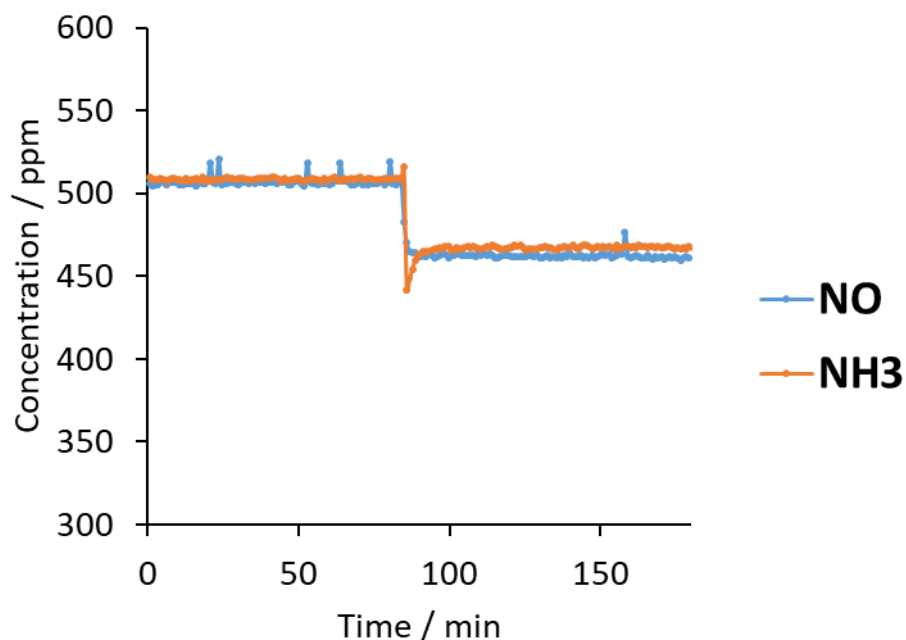


**Figure S23.** Ammonia adsorption when gas stream is sent over a  $\text{CeO}_2$  reactor bed. Initially, the reactor is bypassed and after approximately 80 minutes, the gas stream is sent over the reactor bed. The overshoot of the ammonia concentration upon switching to the reactor indicates that the catalyst adsorbs  $\text{NH}_3$ . Reaction conditions: 210 °C;  $[\text{NO}] = [\text{NH}_3] = 500$  ppm,  $[\text{O}_2] = 10\%$ ; 150 ml/min; 1000 mg  $\text{CeO}_2$ .

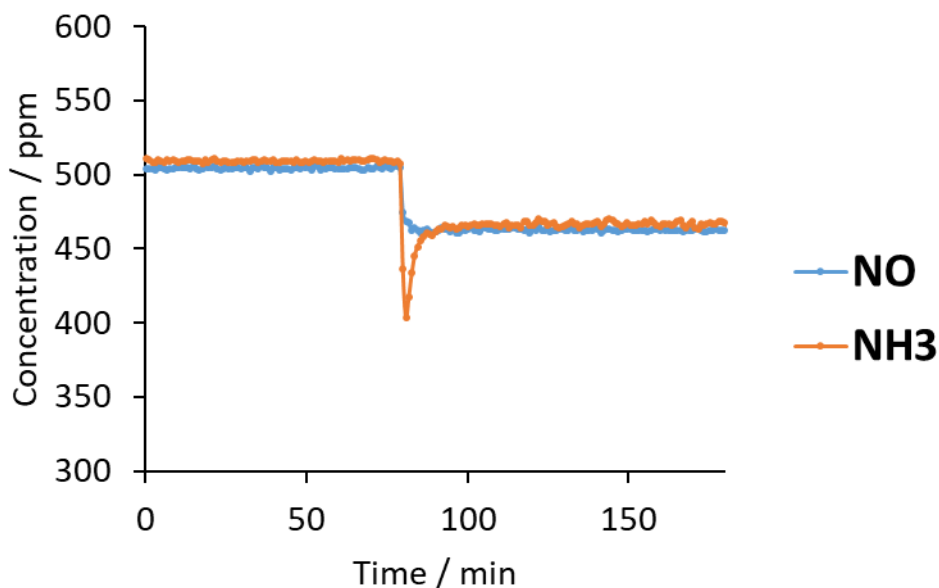


**Figure S24.** Ammonia adsorption when gas stream is sent over a Ce-UiO-66 reactor bed. Initially, the reactor is bypassed and after approximately 70 minutes, the gas stream is sent over the reactor bed. The overshoot of the ammonia concentration upon switching to the reactor indicates that the catalyst adsorbs  $\text{NH}_3$ . Reaction conditions: 210 °C;  $[\text{NO}] = [\text{NH}_3] = 500$  ppm,  $[\text{O}_2] = 10\%$ ; 150 ml/min; 200 mg Ce-UiO-66.

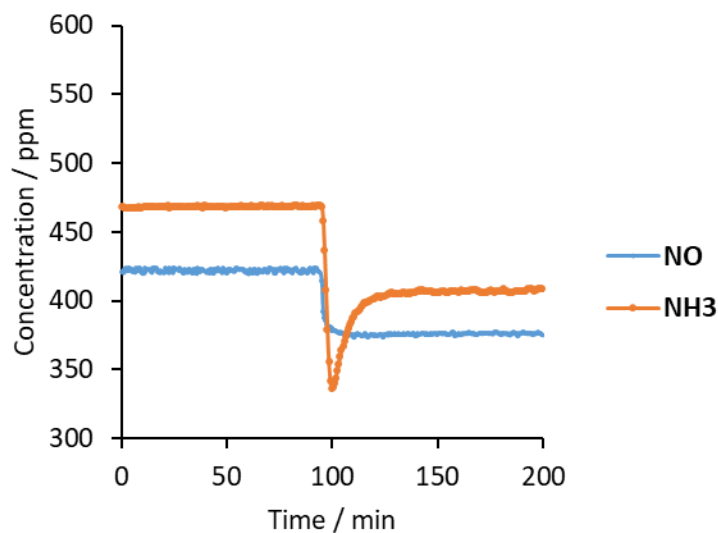


**Figure S25.** Ammonia adsorption when gas stream is sent over a  $\text{Ce}_{10}/\text{Zr-CAU-24}$  reactor bed. Initially, the reactor is bypassed and after approximately 90 minutes, the gas stream is sent over the reactor bed. The overshoot of the ammonia concentration upon switching to the reactor indicates that the catalyst adsorbs  $\text{NH}_3$ . Reaction conditions: 210 °C;  $[\text{NO}] = [\text{NH}_3] = 500$  ppm,  $[\text{O}_2] = 10\%$ ; 50 ml/min; 200 mg  $\text{Ce}_{10}/\text{Zr-CAU-24}$ .

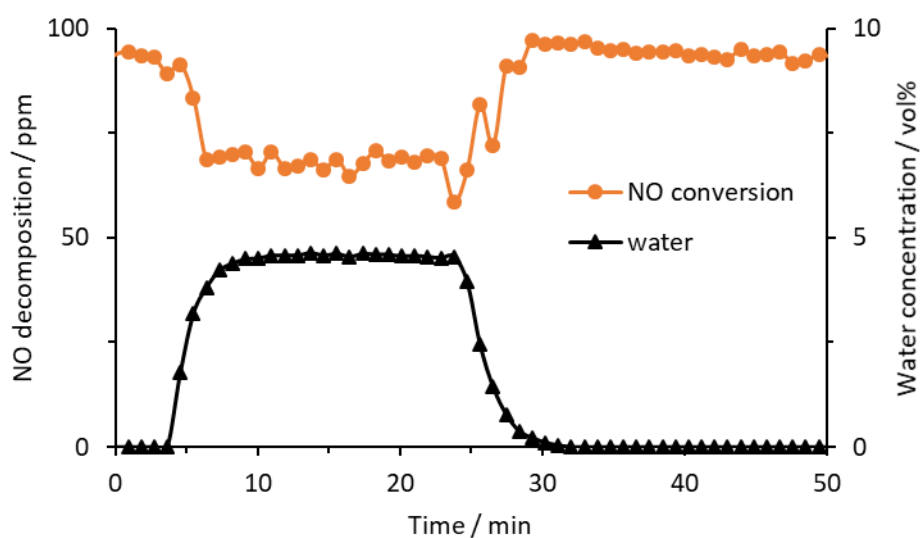


**Figure S26.** Influence of water presence on NO conversion over a  $\text{Ce-UiO-66}$  reactor bed. Reaction conditions: 210 °C;  $[\text{NO}] = [\text{NH}_3] = 500$  ppm,  $[\text{O}_2] = 10\%$ ; 150 ml/min; 200 mg  $\text{Ce-UiO-66}$ .

- (1) Lammert, M.; Wharmby, M. T.; Smolders, S.; Bueken, B.; Lieb, A.; Lomachenko, K. A.; Vos, D. De; Stock, N. Cerium-Based Metal Organic Frameworks with UiO-66 Architecture: Synthesis, Properties and Redox Catalytic Activity. *Chem. Commun.* **2015**, 51, 12578–12581.
- (2) Vermoortele, F.; Bueken, B.; Le Bars, G.; Van de Voorde, B.; Vandichel, M.; Houthoofd, K.; Vimont, A.; Daturi, M.; Waroquier, M.; ... De Vos, D. E. Synthesis Modulation as a Tool to Increase the Catalytic Activity of Metal-Organic Frameworks: The Unique Case of UiO-66(Zr). *J. Am. Chem. Soc.* **2013**, 135, 11465–11468.
- (3) Lammert, M.; Reinsch, H.; Murray, C. A.; Wharmby, M. T.; Terraschke, H.; Stock, N. Synthesis and Structure of Zr(IV)- and Ce(IV)-Based CAU-24 with 1,2,4,5-tetrakis(4-Carboxyphenyl)benzene. *Dalt. Trans.* **2016**, 45, 18822–18826.
- (4) Lammert, M.; Glißmann, C.; Stock, N. Tuning the Stability of Bimetallic Ce(IV)/Zr(IV)-Based MOFs with UiO-66 and MOF-808 Structures. *Dalt. Trans.* **2017**, 46, 2425–2429.
- (5) Rouquerol, J.; Rouquerol, F.; Llewellyn, P.; Maurin, G.; Sing, K. S. W. *Adsorption by Powders and Porous Solids: Principles, Methodology and Applications*; Academic press, **2013**.